Experimental investigation on PFAS degradation through municipal sludge combustion processes

Applied Thermal Engineering 276 (2025) 127006

Contents lists available at ScienceDirect

Applied Thermal Engineering

journal homepage: www.elsevier.com/locate/apthermeng

Research Paper

Experimental investigation on PFAS degradation through municipal sludge combustion processes☆

M. Urciuolo [a], R. Migliaccio [a], B. Ciccone [a,d], G. Ruoppolo [a], A. de Folly d'Auris [b], S. Frisario [c], D. Panepinto [f], G. Premoli [e], B. Ruffino [f], M. Zanetti [f]

[a] Institute of Sciences and Technologies for Energy and Sustainable Mobility, STEMS-CNR, P.le Tecchio 80, 80125 Napoli, Italy
[b] Eni SpA, via Felice Maritano 26, San Donato Milanese, Italy
[c] Eni Rewind SpA, Piazza Boldrini 1, San Donato Milanese, Italy
[d] Department of Applied Science and Technology (DISAT), Politecnico di Torino, C.so Duca degli Abruzzi .24-10129, Torino, Italy
[e] LabAnalysis Environmental Science Srl, via Europa 5, Casanova Lonati, Italy
[f] Department of Environment, Land and Infrastructure Engineering (DIATI), Politecnico di Torino, C.so Duca .degli Abruzzi 24, 10129 Torino, Italy

ARTICLE INFO

Keywords:
PFAS remediation
Municipal sludge
Fluidized bed combustor
Thermal degradation

ABSTRACT

The incineration of sludge matrices at high temperature (>800 °C) represents a valid solution for per- and polyfluoroalkyl substances (PFAS) abatement. The present study investigates the thermal degradation of sludge samples coming from a municipal wastewater treatment plant, by employing a laboratory-scale continuous bubbling fluidized-bed combustor operating at 850 °C and atmospheric pressure. By utilizing samples of raw municipal sludge and spiked with a known PFAS mixture (up to 8 mg/kg), the research could achieve a high analytical sensitivity, enabling a comprehensive evaluation of PFAS combustion efficiency. Preliminary results elucidated the distribution of PFAS molecules within the combustion byproducts, namely flue gases, fly and bottom ashes, shedding light on the PFAS degradation pathways during incineration. The incineration process was characterized by high combustion efficiency (>96 %).

PFAS degradation was always greater than 99.9 % and among them only PFBS, PFOS and PFTeDA were not completely decomposed during the process. The maximum concentration of unconverted PFAS in the flue gas (12 ng/Nm^3) was reduced by 6 orders of magnitude compared to the initial one. Moreover, PFAS concentration within the fly ashes was in the order of 8–18 μg/kg, while it ranged between 1–5 μg/kg in the bottom ashes.

1. Introduction

PFAS (per- and polyfluoroalkyl substances) are a wide family of organic compounds characterized by partial or complete saturation of carbon atoms with fluorine [1]. PFAS can be classified according to different principles, but a convenient distinction is between long-chain PFAS, with typically more than six carbon atoms (e.g., perfluorooctanoic acid (PFOA), perfluorooctanesulfonic acid (PFOS), perfluorotetradecanoic acid (PFTeDA)), and short-chain PFAS, among which perfluorobutanoic acid (PFBA) and perfluorobutanesulfonic acid (PFBS).

The strength of the C-F bond (average bond enthalpy of 486 kJ/mol) makes PFAS molecules suitable for various industrial applications but extremely resistant to degradation [2]. Their use in industry dates back to 1950 s, and today more than 4000 different PFAS are systematically produced and employed worldwide [3]. For instance, they are present in firefighting foams to extinguish flammable liquid fires. In consumer products, PFAS are used to impart non-stick properties to cookware, water and stain resistance to textiles and grease resistance to food packaging (Fig. 1). Additionally, they are utilized in the manufacturing of semiconductors, photographic films, and also in the healthcare sector (surgical fabrics, coatings of some medical products), cleaning sector and in construction materials [4].

Their resistance to degradation and their tendency to bioaccumulation and migration through different solid, liquid and gaseous matrices have raised deep concerns about threats for human beings and for the environment. Growing scientific evidence indicates that exposure to certain PFAS can lead to adverse health outcomes, such as neurodevelopmental disorders, increased risk of thyroid diseases and cancer [5].

PFAS can be transferred from industry to the environment passing

☆ This article is part of a special issue entitled: 'Combustion for Net-Zero' published in Applied Thermal Engineering.

E-mail address: biagio.ciccone@stems.cnr.it (B. Ciccone).

https://doi.org/10.1016/j.applthermaleng.2025.127006
Received 4 March 2025; Received in revised form 20 May 2025; Accepted 28 May 2025
Available online 30 May 2025

Nomenclature

Abbreviations

HTL	Hydrothermal liquefaction
ICP-MS	Inductively Coupled Plasma-Mass Spectrometry
PCB	Polychlorinated biphenyl
PCDD/F	Polychlorinated dibenzo-dioxins/-furans
PFAS	Per- and polyfluoroalkyl substances
PFBA	Perfluorobutanoic acid
PFBS	Perfluorobutanesulfonic acid
PFOA	Perfluorooctanoic acid
PFOS	Perfluorooctanesulfonic acid
PFTeDA	Perfluorotetradecanoic acid

Symbols

n_X	Molar flowrate of component X [mol/h]
Q	Volume flowrate [Nl/h, @0 °C, 1 bar]
V_0	Standard molar volume of ideal gas [Nl/h @STP]
ε	Effective combustion efficiency [-]
ϕ	Excess air [-]

through wastewater treatment plants (WWTP), leading to high PFAS concentrations in the wastewater and in the sludge byproduct (as found in China, the US and Germany [1]). Despite great attention has been devoted to PFAS contamination of water (with regulatory bodies around the world establishing guidelines and restrictive limits for PFAS concentrations in drinking water[1] [6]), less attention has been given to the management of contaminated sludge. In fact, PFAS exhibit a strong tendency to adsorb onto sludge matrices reaching concentrations up to thousands of nanograms per gram of dry weight [1].

In this context, efficient and safe treatment of sewage sludge containing PFAS is of outstanding importance to limit PFAS spread into the environment. Among the different approaches found in the literature (non-thermal, thermal, biological) [5,7,8], thermal routes are emerging as promising methods for PFAS degradation, using high-temperature processes to break down these persistent compounds.

Pyrolysis of contaminated sewage sludge (400–900 °C in O_2-free environment) has been widely explored as viable solution for PFAS abatement in biosolids and simultaneous production of biochar. Recently, Husek et al. (2024) demonstrated that slow-pyrolysis in a stainless steel fixed-bed reactor at temperatures above 400 °C can effectively remove monitored PFAS from sewage sludge [9]. Similar observations have been made in the context of a commercial-scale auger-based pyrolysis unit [10] and in a bench scale mechanically fluidized-bed reactor [11], where no PFAS was detected in the biochar at 700 °C. Nevertheless, the produced gas still contained residual PFAS, suggesting the needing of an oxidation step [12]. McNamara et al. (2023) highlighted that also the resulting bio-oil can contain PFAS [13]. Another interesting investigation on the potentiality of pyrolysis to degrade PFAS was reported by Rathnayake et al. (2025) [14].

Commercial sludge pyrolysis units should operate at temperatures above 500 °C and with residence time at least of 10 min to ensure complete degradation of PFAS in the solid.

Hydrothermal liquefaction (250–350 °C, 10–25 MPa in presence of liquid water, with residence time up to 30 min) was less explored. Yu et al. (2020) concluded that the process can be quite effective in removing fluorinated carboxylic acid structures, but not for sulfonic acid structures [15]. Zhang et al. (2020) investigated HTL to remove PFAAs (perfluoroalkyl acids) from plant biomass, highlighting how high residence time (2 h at 300 °C) can remove PFAAs, while the presence of KOH was necessary to improve the degradation of perfluorosulfonic acids (PFSAs) [16]. Unfortunately, HTL suffers from high costs related to operating pressure and still requires research for scale-up.

Gasification can convert organic materials to syngas in high-temperature conditions (800–1200 °C), but the technological complexity is higher than in combustion processes and PFAS concentration in the residual char can be above limits for its use as soil amendment [17].

Incineration (typically 800–1200 °C) of contaminated sludge is an energy intensive chemical destruction in an oxidizing atmosphere. Compared to other thermal treatments, combustion is a consolidate technology for the management of hazardous materials and can represent a commercial solution to the problem [18]; it already has existing infrastructure and the scaling up of the process is easier. Moreover, mineralization of PFAS compounds into HF and other inorganic F is

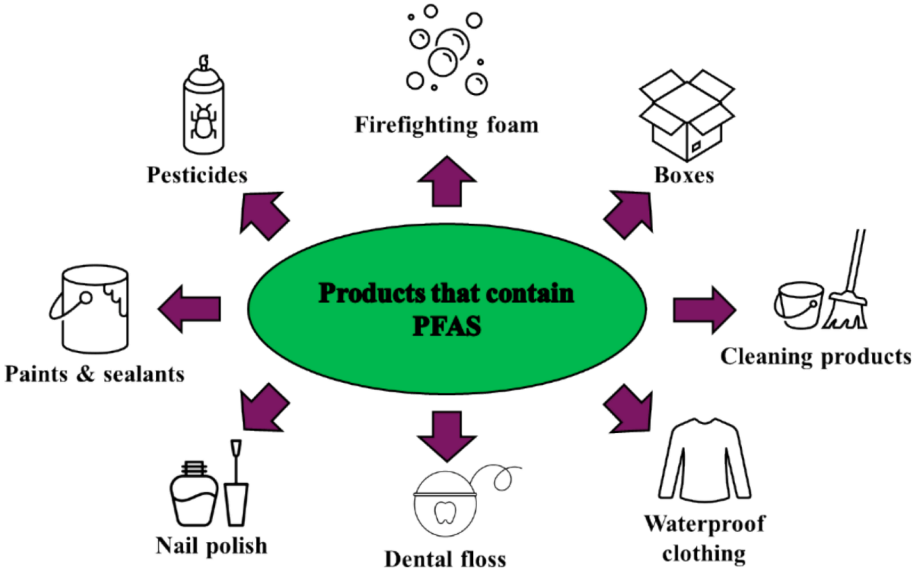

Fig. 1. Industrial applications of PFAS.

[1] In the European Union (EU) total PFAS concentration in drinking water should not exceed 500 ng/L [6].

favoured by the presence of oxygen. Excess oxygen increases the rate of defluorination reactions and improves combustion efficiency [19–21]. Incineration of PFAS waste can generate F-containing pollutants in the gas phase (VOF, HF, COF_2…) that require advanced cleaning technologies [22].

Few studies are available in the literature about destruction of PFAS during incineration on a big scale [19]. Loganathan et al. (2007) reported a PFAS removal efficiency of 50–79 % in biosolids incineration ash residue (for instance, PFOA 17.2 ng/g) compared to the feedstock (80.3 ng/g) [23]. Winchell et al. (2024) [24] extensively examined PFAS-containing sludge incineration in both multiple-hearth furnace (MHF) and fluidized bed furnaces (FBF) on a commercial scale, observing significant PFAS reduction and compositional changes. It is still unclear which technology is superior in terms of PFAS degradation efficiency. Seay et al. (2023) reported variable degradation efficiency for individual PFAS compounds in a sewage sludge incinerator operating at 830 °C and with a residence time of 8 s. Globally, the total PFAS destruction was 51 %, suggesting the necessity of optimizing the operating parameters of the plant to increase PFAS abatement [25].

Some works in the literature are related to muffle oven incineration in the presence of calcium [26] and at different temperatures [27]. Other research has focused on waste combustion, e.g., PFTE [28], fluorotelomer-based polymers [29], contaminated textiles [30]; or on the degradation kinetics of selected PFAS compounds [31,32]. Up to date, systematic observations within fluidized-bed reactors are limited and the mechanism of PFAS degradation is still inadequately understood [33]. Fluidized-bed technology is considered a valuable solution for the thermal treatment of civil and industrial sludge thanks to its ability to guarantee high gas–solid contact (oxygen-PFAS), perfect mixing condition and uniformity of temperature, avoiding hotspots and thermal segregation phenomena. More research is also needed on the fate of PFAS compounds, on the degradation efficiency, on the effect of the operating conditions (temperature, air excess) and on the fluorinate molecules distribution within the combustion flue gas and residual ashes [19].

Results from previous experiences on sludge thermochemical conversion [34–37] have been considered to set up the experimental conditions of this work, aligning with the consideration that the tuning of the most important experimental variables (bed temperature, excess air) is the key factor to control the emission and the efficiency of the process. In this context, Hartman et al. (1999) found that the optimal temperature for dried sewage sludge combustion in a fluidized bubbling combustor is between 850–950 °C, with the freeboard maintained at a minimum of 800 °C for efficient afterburning [38]. Han et al. (2012) explored the effects of moisture levels and feed rates in a fluidized-bed reactor, concluding that pre-drying sludge to below 40 % moisture is crucial for stable combustion [39]. Wet sludge, while reducing bed temperature, helps lower SO_2 emissions and concentrates heavy metals in ash. Lee et al. (2008) reported that dry sludge achieves the highest combustion efficiency with a residence time over 2 s and an air/fuel ratio of at least 5 [40]. Urciuolo et al. (2012) studied the segregation and morphological changes of pelletized wet sludge during combustion, noting that particles fragment during drying but remain stable if they are below a critical size [41].

In this work, the results from a preliminary experimental campaign of sewage sludge combustion are presented. PFAS thermal degradation has been investigated using a laboratory-scale bubbling fluidized bed combustor operated in the typical working condition of a traditional MSW incinerators [8], i.e., at 850 °C and atmospheric pressure, in order to give a contribution to highlight the fate of PFAS during incineration and the effect of air excess on the abatement process. This work provides new evidence on the potential of fluidized bed incineration for effective PFAS destruction in biosolids, supporting its application as a viable technology for managing contaminated sludge in wastewater treatment facilities.

2. Materials and methods

2.1. Fuel characterization

Real sludge samples from a domestic wastewater treatment facility have been spiked with high concentrations of 5 representative PFAS compounds by LabAnalysis S.r.l., a laboratory specialized in PFAS measurements and analysis (see Table 1). It should be noted that the PFAS enrichment of the sludge was necessary to allow adequate analytical sensitivity, given the low concentrations of PFAS present in the sludge as received. Spiked sludge samples had PFAS concentrations surpassing those found in raw sludge by a factor of 100. Three different batches of sludge, collected in different months (May, July, September) have been tested. They will be further indicated as Sample 1, Sample 2 and Sample 3. In particular, Sample 1 was enriched to higher PFAS concentration compared to Sample 3. A batch of as-received sludge (Sample 2) was tested as reference.

The raw sludge was mixed with an aqueous solution containing the desired amount of PFAS to be added. The sludge was kept under stirring for several hours and then dried at ambient temperature up to the required moisture content. After the drying process was completed, the concentration of PFAS in the samples was verified through analytical techniques.

The presence of the 5 PFAS compounds in the sludge samples and in the combustion products (flue gas, fly ashes, bottom ashes) was assessed according to the following standard procedures:

- ASTM D7968-17 − Standard Test Method for Determination of Polyfluorinated Compounds in Soil By Liquid Chromatography Tandem Mass Spectrometry (LC/MS/MS).
- EPA OTM-45 − Measurement of Selected Per- and Polyfluorinated Alkyl Substances from Stationary Sources (duration of the sampling was 120 min, with a flowrate of 6 L/min).

The choice of the specific 5 PFAS compounds used to spike the sludge in this experimental campaign was dictated by the following reasons: i) quick availability of the necessary standards; ii) it is a mixture of PFAS representing different chain length and different terminal functional group; iii) necessity of considering PFAS typically present in real matrices.

The chemical and physical characterization of both the sludge as received and the spiked samples has been performed at the STEMS institute of the National Research Council of Italy. Before analysis, sludge samples have been grinded to make them more homogeneous, since they were available in the form of pasty aggregates varying in size up to a few centimeters. All measurements were repeated at least three times and the statistical mean from the measurements is reported in this work. A representative picture of a sludge sample as received is shown in Fig. 2.

Proximate and ultimate analyses were performed according to ASTM and UNI standards using a LECO TG701 thermogravimetric balance (ASTM D5142), LECO CS144 (ASTM D 4239) and a LECO CHN 628 elemental analyzer (ASTM D5373), respectively. The calorific value was found using a PARR 6200 calorimeter (ASTM D 5865) with a Mahler calorimeter bomb. Metal analyses were performed by *Inductively Coupled*

Table 1
PFAS added to the sludge samples.

Compound	Sample 1 [mg/kg]	Sample 2 [mg/kg]	Sample 3 [mg/kg]
PFBS	1.9	<LOD*	0.2
PFTeDA	1.8	<LOD	0.5
PFOA	1.9	<LOD	1.7
PFBA	2.0	<LOD	2.4
PFOS	1.0	<LOD	0.9
Total PFAS	8.6	<LOD	5.7

*LOD = Limit of detection

Fig. 2. As-received sludge sample.

Plasma-Mass Spectrometry (ICP-MS, Agilent 7500CE) after dissolution of the samples by microwave-assisted acid digestion, in accordance with US-EPA Methods 3051 and 3052. All measurements were repeated at least three times.

2.2. Experimental apparatus and test procedure

The combustion tests have been performed using a laboratory scale bubbling fluidized bed combustor (41 mm ID and 1 m height) at a constant temperature of 850 °C and a fluidization velocity of 0.5 m/s. A windbox (41 mm ID and 600 mm height), placed at the bottom of the reactor, is used to preheat and equalize the fluidizing gas. The gas distributor consists of a metal fabric type Touraille N°FR 35x360 made of AISI 316l steel. On the fluidization column, about 0.5 mm from the distributor and staggered by 180°, are welded two AISI 316 (41 mm ID) through-steel tubes used, respectively, for the continuous fuel feeding and for the measurement and control of the operating pressure and temperature, using a type K thermocouple (1 mm thick), as shown in Fig. 3.

The fuel (sludge) was continuously fed through a mechanical-pneumatic system consisting of a loading hopper positioned on a screw feeder that transports the solid particles into a little jar into which a flow of air pneumatically injects the particles at the base of the bed. For this reason, the fuel was crushed, sieved into small particles (<1 mm), and dried (to a moisture level of ≈5% wt.) to facilitate the feeding process. Both fluidizing air and transport air are supplied by an Atlas-Copco ZE45 screw compressor. The residence time of the gases in the reactor was 2 s, and the air/fuel mass ratio was in the range 5.9–7.5 for all the tests. A metallic filter, kept at 300 °C to avoid water condensation, was used to collect elutriated sand or biomass particles. As schematized in Fig. 3, a fraction of the flue gases was sent to the online gas sampling and analysis system, while the rest was sent to the vent.

The gas sampling and analysis system consisted of a set of on-line ABB analyzers for the continuous measurement of O_2, CO_2, CO, NO_x and SO_2; moreover, a dedicated sampling system has been set up for organic contaminants, namely PFAS, PCDD/F and PCB. All gas sampling has been performed in steady state conditions. At the end of each test, the determination of the analytes of interest in the ash (those collected in the filter, henceforth called "fly ash", and those in the bed of the reactor,

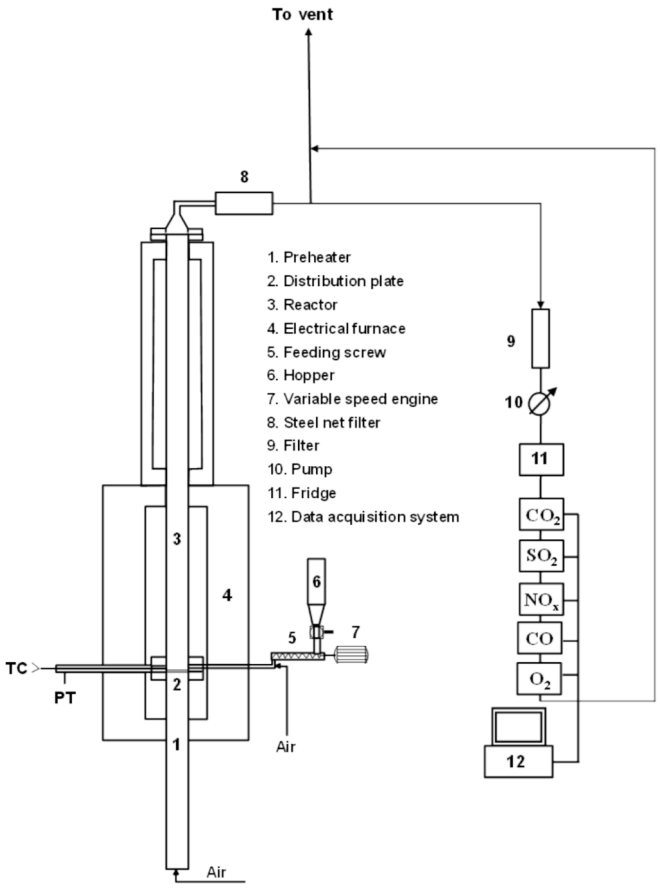

Fig. 3. Laboratory scale fluidized bed combustor used in the experimental campaign.

"bottom ash") and in the condensed smoke was performed by LabAnalysis S.r.l. The main properties of the silica sand used as bed material are reported in Table 2.

For all experimental tests performed, the test protocol adopted sequentially included:

- Preheating of the fluidized bed reactor using electric furnaces until reaching the operating temperature inside the bed of approximately 850 °C.
- Adjustment of combustion air and sludge flow rate to the combustor until the achievement of stable oxygen concentration in the flue gas between 4 and 7 % vol.
- Verification of achievement of steady-state operating conditions, by monitoring gaseous emissions at the reactor outlet (specifically, CO_2 and O_2).
- Sampling of PFAS/total fluorine/PCDD/F and VOCs in the gaseous stream, downstream of the filter; in order to sample a detectable amount of pollutant, the duration of steady-state operation was typically 2–4 h, estimated on the base of the mass balance of the contaminant added to the feed.

Table 2
Properties of the reactor fluidizing material.

Properties of the bed material (silica sand)	
Granulometry, mm	0.3–0.4
Sauter diameter, mm	0.35
Minimum fluidization velocity (at 1123 K), m/s	0.044
Terminal velocity (at 1123 K), m/s	2.34

- Continuous determination of the main gaseous species (O_2, CO_2, CO and NO_x) in the stream at the outlet from the filter, during the entire duration of the test.
- Shutdown of the combustor, cooling down to room temperature under air flow, product recovery and analysis.

Table 3 illustrates the experimental conditions of the combustion tests, particularly referring to the fuel feed rate and excess of combustion air. Four tests were conducted using sludge Sample 1, with constant gas velocity while varying the air excess (ranging from 12 to 26) to evaluate the effect of this parameter on the decomposition and distribution of PFAS. A single test was performed with the sludge collected in July (Sample 2), with a significantly higher air excess (54). Additionally, four tests were conducted using Sample 3: two with an air excess similar to that used for Sample 2, aimed at assessing the impact of feedstock variability, and two with a substantially higher air excess (62–65). The tests were performed feeding around 100–120 g/h of sludge, with a total thermal power of 0.4–0.5 kW_{th}, which is consistent with the laboratory scale size.

Sampling of gas for PFAS detection and measurement has been performed by LabAnalysis S.r.l. through the dedicated sampling apparatus illustrated in Fig. 4. Sampling of PFAS/total fluorine/PCDD/F and VOCs in the gaseous stream, downstream of the filter, carried out during steady-state of the combustor, was performed for 2–4 h, the time interval necessary to sample a sufficient amount for analysis.

The sampling system installed at the outlet of the fluidized-bed combustor consisted of a condensate collection system followed by a capture equipment made up of XAD adsorbent material.[2] In addition to the continuous sampling of the flue gas, samples of fly ashes and bottom ashes were also retrieved for further analytical characterization.

3. Results and discussion

3.1. Fuel characterization

The representative characteristics of the dry sludge used in the three sessions of the experimental campaign are reported in Table 4. Comparison of the results of the analysis on the different samples shows that the sludges have almost the same composition (except for the higher fixed carbon content and lower ash content of Sample 1 compared to the other sludges), agreeing with the consideration that they are sludge samples from the same site but collected at different times of the year.

The ICP-MS analysis showed high concentration of some elements, especially Fe (≈4%wt.), P (≈ 3 %wt.) and Ca (≈ 2 %wt.). The presence of these components can strongly influence combustion behavior. It is reported that the combustion of Fe, P and Ca-containing sludge can lead to slag formation due to iron and potential corrosion problems from phosphorus emissions [35,42]. Nevertheless, iron has shown potential to act as metal catalyst for PFAS degradation by easing the C-F bond cleavage [43]. Calcium has been shown to have the ability to bind PFAS to the surface of combustion ashes, regardless of the chain length [26].

3.2. Incineration tests

Tests from N°1 to N°4 were performed using a lower excess air (20–30 %) compared to tests with Sample 2 and 3 (around 50–60 %). Table 5 reports the main results from the incineration tests, namely the effective combustion efficiency, the mean composition of the flue gas in steady state conditions, flowrate and concentration of fly and bottom ashes.

The difference in excess air significantly influenced the combustion efficiency in terms of pollutant emissions and ash recovery from the combustor. For all tests, a stable steady state was easily reached, and it was maintained during all the measurement, as it is possible to see from the concentration profiles of O_2 and CO_2 obtained during test N°5 (Fig. 5). Only carbon monoxide (CO) exhibited a more oscillatory behavior, which could be associated with its sensitivity to incomplete combustion, non-linear reaction kinetics and local variations in temperature, or to a not well-developed fuel–air mixing which promote the formation of rich combustion condition.

In contrast, CO_2, as the stable end product of combustion, remains more steady and less affected by transient changes [44]. The repeatability of the experiments is confirmed by the O_2 content in the flue gas from the combustion process, which was similar for tests conducted under the same excess air (ϕ) conditions, e.g., an O_2 content of roughly 4 % for tests with Sample 1, and 7 % for Sample 2 and 3.

From Table 5 it can be noted that higher O_2 content in the reactor resulted in a reduction in CO and NO_x production from 2500-3000 ppm to 1100–1300 ppm and from 2500-3200 ppm to 1000–1600 ppm, respectively. This is a result of the enhanced combustion efficiency, which leads to a more complete oxidation of the bio-solid. As expected, given the high concentrations of fly ashes and of NO_x in the flue gas and the significant production rate of fly ash, it is necessary foresee additional processes and technologies to reduce solid and gaseous emissions from the combustion process. The expression of combustion efficiency adopted in this work is shown in Equation 1:

$$\varepsilon = \frac{n_{out} - n_{CO} - n_{CH4} - n_{Csolid}}{n_{out}} \quad (1)$$

where ε is the net combustion efficiency, n_{out} is the total carbon molar flow at outlet (namely the sum of all carbon flows with the flue gas and with the solid residues), n_{CO}, n_{CH4} and n_{Csolid} are the molar flows of carbon related to CO, CH_4 and char. This parameter is used to quantify carbon effective combustion to carbon dioxide (CO_2) as product, which is a sign of clean and efficient combustion. According to the definition of Eq. 1, a 100 % efficient combustion would produce only CO_2, with a solid residue containing negligible traces of carbon.

In practical processes, due to incomplete or ineffective oxidation and poor local mixing between fuel and oxygen, other carbon-containing products are generated, such as carbon monoxide and methane. Furthermore, carbon can be left unburned within the solid matrix. As expected, the combustion efficiency is lower when the excess of oxygen is lower (tests N°1 to N°4). Nevertheless, the combustion efficiency was generally higher than 96 %, given the low carbon content of the residual ash collected in the filter. This result confirms the high reactivity of the material under investigation. The testing time has been set to 4 h, except for tests N°6 and N°7 which lasted for 90 min. This duration was necessary to ensure that a significant amount of PFAS compounds and other analytes could be sampled and assessed with reasonable accuracy. The fly ash concentration and their carbon content are comparable to values obtained in other experiments [35].

As shown in Table 5, the fly ash rate is slightly higher in tests on session 1 compared to other sessions. Higher fly ash rates with lower O_2 excess result from incomplete combustion, where insufficient oxygen leads to more unburned fuel and residues being carried away as fly ash. In tests where Sample 1 was used, the fly ash represents around 8–11 % of the feed, and the bottom ash is 8–14 % on a mass basis. For the tests with Sample 3, fly ash and bottom ash represent 4–8 % and 19–22 % of the feed, respectively.

3.3. PFAS abatement and partitioning

Fig. 6 illustrates the mass distribution of total PFAS as a function of excess air for three different experimental runs, namely test N°3 (ϕ = 12

[2] XAD adsorbent material refers to a family of synthetic, highly porous polymeric resins developed primarily by Rohm and Haas (part of Dow Chemical). These materials are used as adsorbents for various applications, particularly in the separation and purification of organic compounds from aqueous solutions.

Table 3
Operating conditions for the experimental tests.

	Sample 1				Sample 2	Sample 3			
Test N°	**N°1**	**N°2**	**N°3**	**N°4**	**N°5**	**N°6**	**N°7**	**N°8**	**N°9**
Feed rate, g/h	119.7	115.5	126.8	113.2	102.9	103.6	101.1	103.4	99.3
Power, kW_{th}	0.491	0.474	0.533	0.476	0.379	0.387	0.378	0.386	0.371
Air excess, %	18	22	12	26	54	58	62	58	65
Air/fuel ratio [g/g]	6.26	6.49	5.91	6.62	7.29	7.24	7.42	7.26	7.56

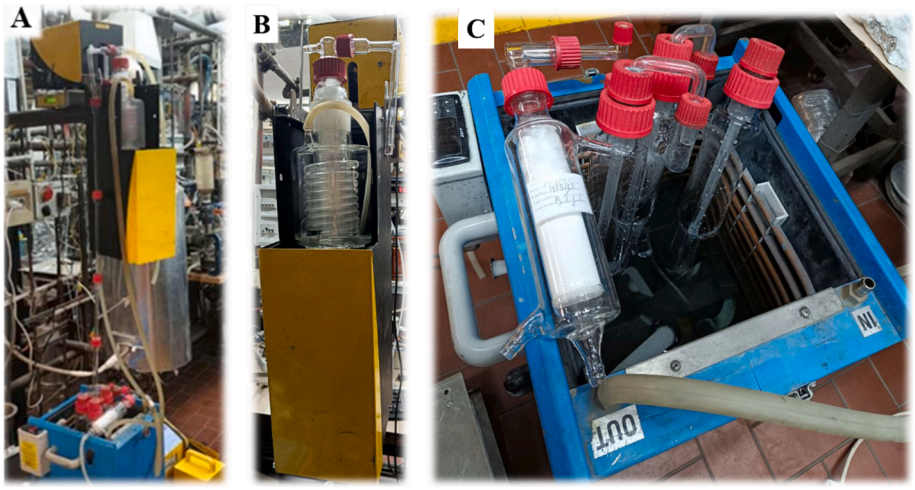

Fig. 4. Set-up for PFAS sampling (A), with condensate collection equipment (B) and capture system made up of adsorbent XAD material (C).

Table 4
Proximate and ultimate analyses of the sludge samples (as received, %wt).

Analysis	Sample 1	Sample 2	Sample 3
Moisture	4.7 ± 0.1	5.7 ± 0.03	4.5 ± 0.4
Volatiles	65.3 ± 2.0	59.3 ± 0.1	61.3 ± 1.6
Fixed carbon	8.1 ± 0.4	4.9 ± 0.03	4.9 ± 0.1
Ash	21.9 ± 2.5	30.2 ± 0.1	29.4 ± 1.9
Carbon	36.2 ± 1.3	32.6 ± 1.6	31.6 ± 0.4
Hydrogen	5.4 ± 0.3	4.7 ± 0.2	4.6 ± 0.1
Nitrogen	5.7 ± 0.2	5.1 ± 0.4	6.1 ± 0.9
Sulfur	0.98 ± 0.4	0.89 ± 0.01	0.96 ± 0.04
Chlorine	0.12 ± 0.03	0.033 ± 0.02	0.075 ± 0.011
Fluorine	0.018 ± 0.002	0.0053 ± 0.0037	0.0112 ± 0.001
Oxygen (by difference)	25.0 ± 1.9	20.8 ± 2.1	22.8 ± 1.1
LHV [kJ/kg]	15139 ± 243	13122 ± 13	13457 ± 33

%), N°8 ($\phi = 58$ %) and N°9 ($\phi = 65$ %), respectively. The total PFAS input to the system has been a result of the enrichment operation described previously and reported in Table 1.

The destruction of PFAS molecules is almost complete in all the air excess conditions explored, as shown by the red line in Fig. 6. Less than 0.06 % of total PFAS entering the system is surviving thermal treatment, with negligible differences with changing excess air (0.026 % at $\phi = 12$ %, 0.052 % when $\phi = 58$ % and 0.034 % at $\phi = 65$ %). As illustrated by the dashed line of Fig. 6, more than 90 % of the PFAS surviving the incineration is concentrated within the ash (i.e., both bottom and fly ashes), while only less than 8 % is left behind as flue gas emissions in the worst case. The sequestration of PFAS compounds in the bottom ashes, which are a solid residue not representing an emission source (if adequately treated), is maximum when $\phi = 58$ %. The distribution of PFAS in the bottom ashes follows a non-monotonic trend (with a maximum at $\phi = 58$ %), while the opposite trend is found for fly ashes. When $\phi = 58$ %, the survived PFAS (by mass) are mostly sequestered in the ashes, with 86.8 % being collected in the bottom ashes and the remaining 12.8 % in the fly ashes. PFAS emissions within the flue gas represent only 0.45 % of the surviving PFAS, which, as discussed earlier, are in turn 0.052 % of the initial amount of the spike.

Fig. 7 shows the effect of excess air (ϕ) on the concentration of selected PFAS compounds within the flue gas sampled at the exit of the

Table 5
Main results from the sludge incineration tests.

	Sample 1				Sample 2	Sample 3			
Name	N°1	N°2	N°3	N°4	N°5	N°6	N°7	N°8	N°9
Combustion efficiency, %	96.4	96.3	96.3	95.5	99.2	98.94	98.96	99.02	98.86
Mean composition of flue gas v/v.									
O_2, %	3.89	4.07	4.21	4.88	7.44	7.37	6.39	6.79	6.95
CO_2, %	14.19	13.98	14.32	13.27	11.88	11.14	12.00	11.72	11.56
CO, ppm	2801	2871	2506	2614	948	1178	1243	1122	1306
NO_x, ppm	2900	3200	2500	2700	1506	1000	1174	1487	1608
Flowrate and concentration of ash									
Fly ash, g/h	10.12	10.74	14.57	10.84	6.5	4.8	5.93	8.55	8.03
Carbon in Fly ash, g/h	0.019	0.03	0.168	0.146	0.008	0.006	0.007	0.01	0.01
Fly Ash concentration, mg/Nm^3	17,451	18,519	25,123	18,686	11,247	8266	10,220	14,742	13,845
Bottom ash, g/h	17.3	17.0	10.7	13.4	13.5	23.1	19.3	21.1	22.6

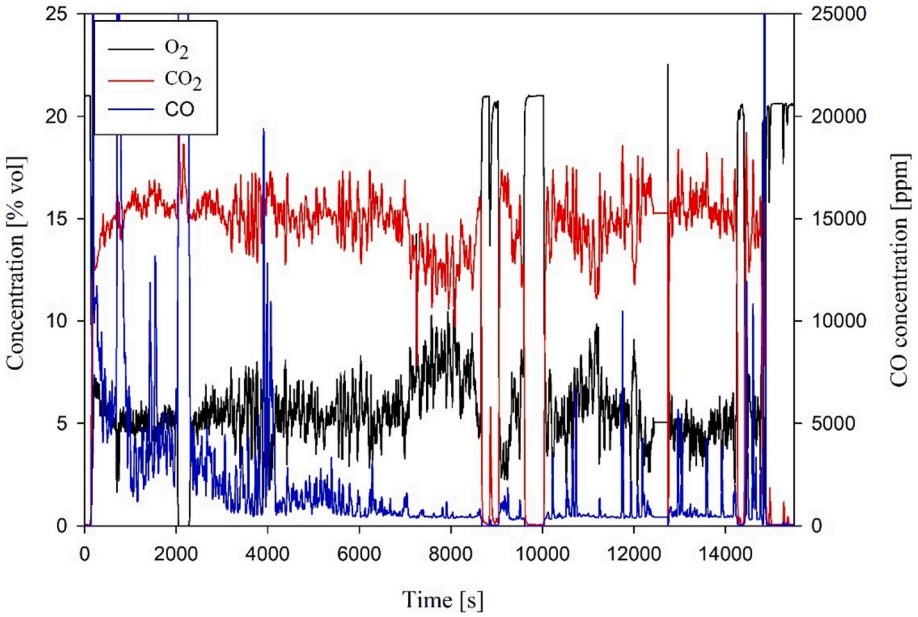

Fig. 5. Time series of CO_2, O_2 and CO concentration (test N°5, $\phi = 54$ %, T = 850 °C).

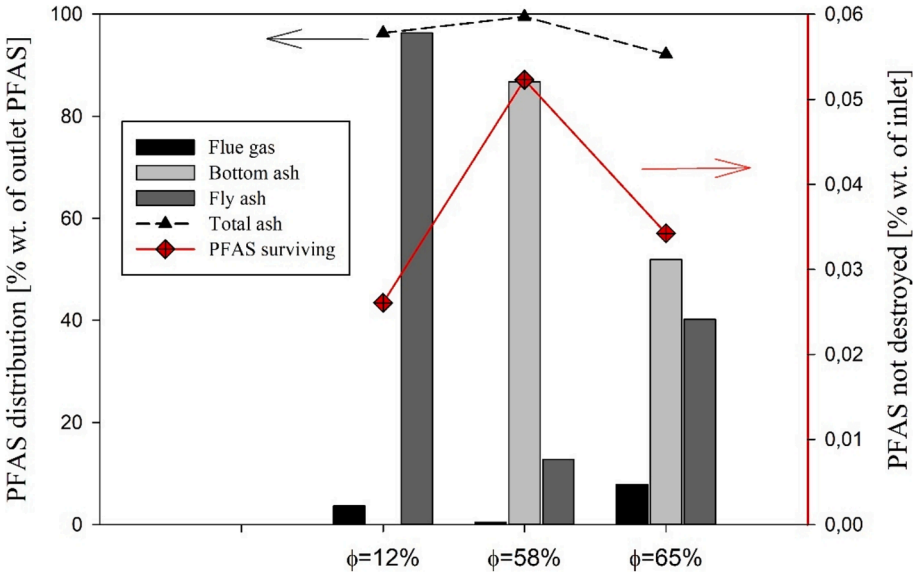

Fig. 6. PFAS distribution within ashes and flue gas and PFAS survived.

reactor. The concentrations of three specific PFAS compounds—PFBS (perfluorobutanesulfonic acid), PFOS (perfluorooctanesulfonic acid), and PFTeDA (perfluorotetradecanoic acid)—were measured successfully in the flue gas, while PFOA (perfluorooctanoic acid) and PFBA (perfluorobutanoic acid) remained undetected under all conditions. PFBS was detected only when the air excess was low (12 %) with a concentration reduced of 6 orders of magnitude compared to the initial one (10.7 ng/Nm^3),[3] while it was completely abated during tests with higher excess air (58 % and 65 %). On the other hand, PFOS and PFTeDA appeared to be completely destroyed in lower excess air conditions, while surviving in air-rich conditions.

More in detail, PFOS was not detected at 12 % excess air but began to appear in the flue gas at higher excess air levels, with concentrations increasing from 0.79 ng/Nm^3 at 58 % excess air to 7.1 ng/Nm^3 at $\phi = 65$ %. Similar conclusions may be drawn for PFTeDA (0.9 ng/Nm^3 at $\phi =$ 58 %, and 12 ng/Nm^3 at $\phi = 65$ %). The absence of PFOA and PFBA in the flue gas is an interesting result, particularly because PFOA is a longer-chain PFAS known for its thermal stability. Its absence suggests that under the combustion conditions used in this study, PFOA may have been partly degraded in the fluidized bed reactor and partly sequestered in other solid residues such as fly ash or bottom ash (as will be discussed further on). For PFBA, the short-chain structure likely contributed to its complete decomposition under these thermal treatment conditions, similar to PFBS.

To allow for a proper comparison between the three tests, the ratio of the total PFAS concentration in the flue gas to the initial spike concentration in the sludge sample (namely, $ng/kg_{gas}/ng/kg_{sludge}$) has been chosen as parameter. As illustrated in Fig. 7, the concentration ratio follows a non-monotonic trend, which exhibits a minimum when the air

[3] The concentration has been normalized to the reference concentration of O_2 of 11% vol., which is the typical O_2 concentration of an industrial incinerator (as requested by the D.Lgs. 152/06).

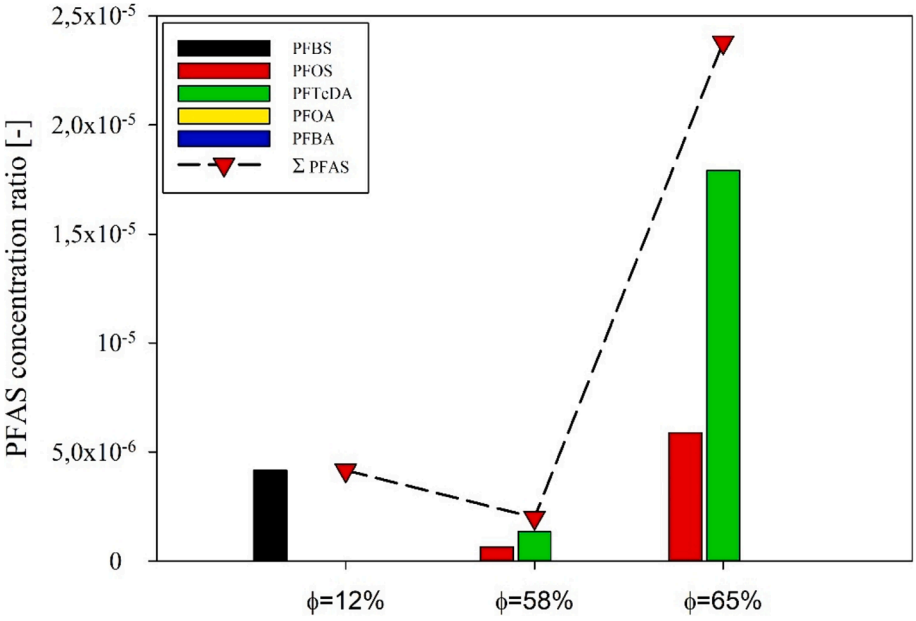

Fig. 7. Ratio of PFAS concentration in the flue gas to the initial concentration in the sludge [ng/kg_{gas}/ng/kg_{sludge}] as function of excess air.

excess is 58 %. For short-chain PFAS (like PFBS), increasing the air excess promotes their complete degradation, while for long-chain PFAS (like PFOS and PFTeDA), higher excess air appears to result in incomplete combustion and an increase in emissions in the flue gas. In all the conditions, the concentration ratio is always in the order 10^{-6}–10^{-5}, highlighting efficient degradation.

Looking at the concentration of selected PFAS compounds within the fly ashes (Fig. 8), it can be seen that PFBS concentrations showed a sharp increase as the air excess increased from 12 % to 58 %, followed by a slight increase at 65 %. According to the results, as the air excess increases, more PFBS is likely oxidized in the combustion chamber, reducing its presence in the fly ash. This behaviour aligns with the general trend observed in flue gas data, where PFBS concentration dropped to zero at higher air excess ratios, indicating more complete decomposition in the flue gas phase and subsequent capture in ash residues. PFTeDA concentrations followed a similar pattern to PFBS.

PFOS concentrations exhibited a sharp decline as the air excess increased from 12 % to 58 %, followed by a moderate rise at 65 %. The high concentration of PFOS at 12 % air excess suggests incomplete oxidation, leading to its capture in the fly ash. PFOA concentrations increased consistently with the rising air excess ratio, indicating that incomplete combustion at higher oxygen levels may have led to the persistence of this long-chain PFAS in fly ash.

The absence of PFBA in the fly ash is consistent with the observations from the flue gas data, where this short-chain PFAS was not detected. This suggests that PFBA undergoes complete decomposition under the thermal conditions in the fluidized bed reactor, regardless of the excess air. The data from fly ash suggest that short-chain PFAS like PFBS are more susceptible to complete thermal degradation, as their concentrations generally decrease with increasing air excess.

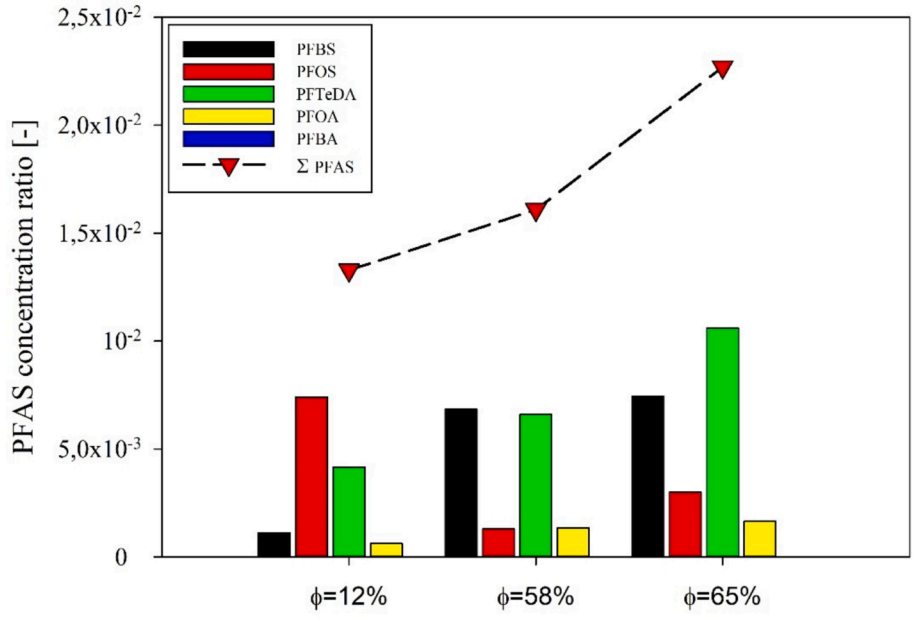

Fig. 8. Ratio of PFAS concentration in the fly ashes to the initial concentration in the sludge [ng/kg_{ash}/ng/kg_{sludge}] as function of excess air.

The concentration of PFAS in the bottom ashes follows a non-monotonic trend with respect to air excess, with a maximum concentration at $\phi = 58$ % (Fig. 9). In low excess air conditions ($\phi = 12$ %), no PFAS was detected in the bottom ashes, while their concentration increased with increasing ϕ to 58 % and then decreased at $\phi = 65$ %. PFBS and PFBA were not detected in the bottom ash under any of the air excess conditions. This is consistent with the trends observed in the flue gas and fly ash data, where PFBS concentrations dropped significantly with increased air excess, indicating its efficient thermal decomposition and PFBA was never detected. PFOA was absent in the bottom ash at 12 % air excess but appeared at 1870 ng/kg (concentration ratio of $1.1 \cdot 10^{-3}$) with 58 % air excess and then decreased to 590 ng/kg (concentration ratio of $3.5 \cdot 10^{-4}$) at 65 %.

This trend suggests that at higher excess air ratios, incomplete combustion allows PFOA to persist and accumulate in the bottom ash. This behaviour is consistent with the findings in the fly ash, where PFOA concentrations also increased at higher air excess ratios, further reinforcing the hypothesis that long-chain PFAS are less efficiently degraded under these conditions. PFOS followed a similar trend to PFOA, with no detection at 12 % air excess, followed by a maximum concentration at $\phi = 58$ %. The concentration then decreased from 1250 ng/kg (concentration ratio of $1.4 \cdot 10^{-3}$) at 58 % air excess to 550 ng/kg (concentration ratio of $6.1 \cdot 10^{-4}$) at $\phi = 65$ %. Similar trends are followed also by PFTeDA, but this species survived with higher concentrations compared to the others, probably due to the stability of the long chain.

Results clearly show that the maximum sequestration level of PFAS within the bottom ashes occurs at intermediate air excess ration (58 %). Increasing or decreasing the excess air leads to an increase in the PFAS emissions through fly ashes and/or flue gas. Again, it should be noted that the concentration of PFAS is reduced by a factor of 1000.

In order to consider the possibility of formation of different, smaller F-containing species coming from the decomposition of PFAS at high temperatures (shorter chain PFAS, HF, fluorinated hydrocarbons…), other 31 PFAS compounds have been monitored during the experimental tests. Nevertheless, none of these was detected in the residual ashes and in the flue gas from the reactor.

The total PFAS degradation was always greater than 99.9 %, with negligible increase with excess air conditions. This suggests that the PFAS degradation and mineralization may be limitedly influenced by the oxidation environment, while being dependent on the combustion temperature and the duration of the thermal treatment [27]. From comparison with the literature [25], we found that some PFAS have comparable removal efficiencies, while others have a different removal efficiency. This is probably due to the different scale of the plant; moreover, while in this work removal efficiency was calculated considering streams entering and exiting from the combustor only, in the work of Seay et al. [25] all influents and effluents from the SSI and the corresponding treatment plant (venturi scrubber, mercury scrubber and others) were considered, making the direct comparison on single PFAS not straightforward. As general comparison, PFAS content between the sludge and the ash residue was reduced 2–10 times in [23], and 7 times in [25]. In this work, we obtained a 100-fold concentration reduction in the solid phase, and a 50000-fold reduction in the gas phase.

The high PFAS abatement registered in these tests at 850 °C is interesting because it shows the possibility of abating PFAS also at temperatures below those commonly reported in the literature (i.e., >1000 °C) for thermal processing of PFAS-contaminated materials [21].

4. Conclusions and future work

Combustion of sewage sludge samples spiked with a known amount of 5 different PFAS compounds (namely, PFOS, PFOA, PFBA and PFTeDA) was investigated using a fluidized bubbling bed combustor operated at 850 °C and atmospheric pressure, working with a mean residence time of 2 s and with air/fuel ratios of 5–7. The experimental campaign aimed to assess the efficacy of the combustion process for the abatement of persistent PFAS compounds and to investigate the fate of PFAS and their partition into the flue gas and to the solid residues (ash), taking into account the effect of air excess within the combustion chamber. Lab-scale tests were performed varying the O_2 concentration in the flue gas between 4–7 % and with a thermal power of 400–500 W. Preliminary results showed that the mean PFAS degradation was always greater than 99.9 %. Only PFBS, PFOS and PFTeDA were not completely decomposed during the process. Nevertheless, unconverted PFAS were poorly present in the flue gas, with a maximum concentration reduced of 6 orders of magnitude compared to the initial one (12 ng/Nm^3). Moreover, PFAS concentration within the fly ashes was in the order of 8–18 μg/kg, while it ranged between 1–5 μg/kg in the bottom ashes. Preliminary results show that incineration of PFAS-contaminated sludge

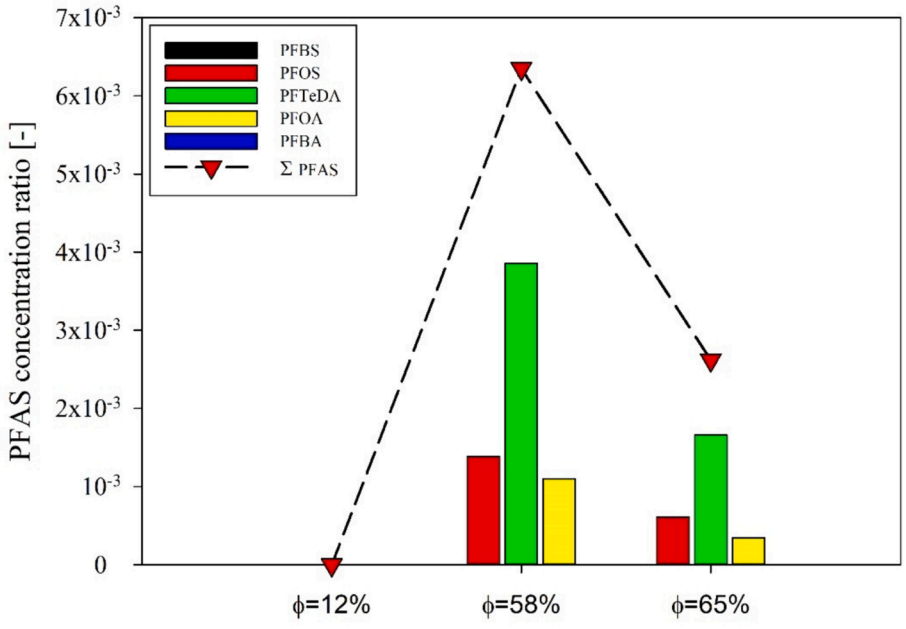

Fig. 9. Ratio of PFAS concentration in the bottom ashes to the initial concentration in the sludge [$ng/kg_{ash}/ng/kg_{sludge}$] as function of excess air.

within a fluidized bed reactor operating at 850 °C could efficiently degrade and/or retain PFAS. Future work will get deeper into the analysis of the degradation mechanism of PFAS compounds, also considering the assessment of the fluorine mass balance across the combustor and the evaluation of harmful emissions (e.g., VOCs, HF, dioxins).

Declaration of competing interest

The authors declare that they have no known competing financial interests or personal relationships that could have appeared to influence the work reported in this paper.

Acknowledgments

The Authors thank the iENTRANCE@ENL: Infrastructure for Energy TRAnsition aNd Circular Economy @ EuroNanoLab Project (Award Number: 128 dated 21/06/2022 – Project Code: IR0000027 -) funded under the National Recovery and Resilience Plan (NRRP), Mission 04 Component 2 Investment 3.1 – NextGenerationEU, Call for tender n. 3264 dated 28/12/2021 for supporting the PhD grant of Biagio Ciccone.

Data availability

No data was used for the research described in the article.

References

[1] T. Zhou, X. Li, H. Liu, S. Dong, Z. Zhang, Z. Wang, J. Li, L.D. Nghiem, S.J. Khan, Q. Wang, Occurrence, fate, and remediation for per-and polyfluoroalkyl substances (PFAS) in sewage sludge: a comprehensive review, J. Hazard. Mater. 466 (2024), https://doi.org/10.1016/j.jhazmat.2024.133637, 133637.

[2] D. O'Hagan, Understanding organofluorine chemistry. An introduction to the C–F bond, Chem. Soc. Rev. 37–2 (2008) 308–319, https://doi.org/10.1039/B711844A.

[3] Y. Pan, J. Wang, L.W.Y. Yeung, S. Wei, J. Dai, Analysis of emerging per-and Polyfluoroalkyl substances: progress and current issues, TrAC Trends Anal. Chem., 124 (2020) 115481, https://doi.org/10.1016/j.trac.2019.04.013.

[4] J. Glüge, M. Scheringer, I.T. Cousins, J.C. DeWitt, G. Goldenman, D. Herzke, R. Lohmann, C.A. Ng, X. Trier, Z. Wang, An overview of the uses of per-and polyfluoroalkyl substances (PFAS), Environ. Sci. Process Impacts 22 (12) (2020) 2345–2373, https://doi.org/10.1039/D0EM00291G.

[5] S.P. Lenka, M. Kah, L.P. Padhye, A review of the occurrence, transformation, and removal of poly-and perfluoroalkyl substances (PFAS) in wastewater treatment plants, Water Res. 199 (2021) 117187, https://doi.org/10.1016/j.watres.2021.117187.

[6] Directive (EU) 2020/2184 of the European Parliament and of the Council of 16 December 2020 on the quality of water intended for human consumption (recast) (OJ L 435, 23.12.2020, pp. 1-62).

[7] I. Ross, J. McDonough, J. Miles, P Storch, P. Thelakkat Kochunarayanan, E. Kalve, J. Hurst, S.S. Dasgupta, J. Burdick, A review of emerging technologies for remediation of PFASs, Remediat. J., 28:2 (2018) 101-126. DOI: 10.1002/rem.21553.

[8] A. Garg, N.P. Shetti, S. Basu, M.N. Nadagouda, T.M. Aminabhavi, Treatment technologies for removal of per-and polyfluoroalkyl substances (PFAS) in biosolids, Chem. Eng. J. 453 (2023) 139964, https://doi.org/10.1016/j.cej.2022.139964.

[9] M. Hušek, J. Semerád, S. Skoblia, J. Moško, J. Kukla, Z. Beňo, M. Jeremiáš, T. Cajthaml, M. Komárek, M. Pohořelý, Removal of per- and polyfluoroalkyl substances and organic fluorine from sewage sludge and sea sand by pyrolysis, Biochar 6 (2024) 31, https://doi.org/10.1007/s42773-024-00322-5.

[10] E.D. Thoma, R.S. Wright, I. George, M. Krause, D. Presezzi, V. Villa, W. Preston, P. Deshmukh, Ph. Kauppi, P.G. Zemek, Pyrolysis processing of PFAS-impacted biosolids, a pilot study, J&AWMA 72–4 (2022) 309–318, https://doi.org/10.1080/10962247.2021.2009935.

[11] H. Bamdad, S. Papari, E. Moreside, F. Berruti, High-temperature pyrolysis for elimination of per- and polyfluoroalkyl substances (PFAS) from biosolids, Processes 10–11 (2022) 2187, https://doi.org/10.3390/pr10112187.

[12] S. Kundu, S. Patel, P. Halder, T. Patel, M.H. Marzbali, B.K. Pramanik, J. Paz-Ferreiro, C.C. de Figueiredo, D. Bergmann, A. Surapaneni, M. Megharaj, K. Shah, Removal of PFASs from biosolids using a semi-pilot scale pyrolysis reactor and the application of biosolids derived biochar for the removal of PFASs from contaminated water, Environ. Sci.: Water Res. Technol. 7 (2021) 638–649, https://doi.org/10.1039/d0ew00763c.

[13] P. McNamara, M.S. Samuel, S. Sathyamoorthy, L. Moss, D. Valtierra, H. Cortes Lopez, N. Nigro, S. Somerville, Z. Liu, Pyrolysis transports, and transforms, PFAS from biosolids to py-liquid, Environ. Sci.: Water Res. Technol. 9 (2023) 386–395, https://doi.org/10.1039/d2ew00677d.

[14] N. Rathnayake, A.K. Sivaram, I.G. Hakeem, S. Pabba, S. Patel, R. Gupta, K. Shah, The fate of per-and polyfluoroalkyl substances (PFAS) during pyrolysis and co-pyrolysis of biosolids with alum sludge and wheat straw, J. Anal. Appl. Pyrolysis 187 (2025) 106970, https://doi.org/10.1016/j.jaap.2025.106970.

[15] J. Yu, A. Nickerson, Y. Li, Y. Fang, T. J. Strathmann, Fate of per-and polyfluoroalkyl substances (PFAS) during hydrothermal liquefaction of municipal wastewater treatment sludge, Environ. Sci.: Water Res. Technol., 6(5) (2020) 1388–1399, doi:10.1039/c9ew01139k.

[16] W. Zhang, H. Cao, S. Mahadevan Subramanya, P. Savage, Y. Liang, Destruction of Perfuoroalkyl Acids Accumulated in Typha latifolia through Hydrothermal Liquefaction, ACS Sustainable Chem. Eng. 8 (2020) 9257–9262, https://doi.org/10.1021/acssuschemeng.0c03249.

[17] Logan City Council, Technical Report for Loganholme Wastewater Treatment Plant: Biosolids Gasification Demonstration Plant (PBE-075), Loganholme Council, Queensland, 2021. https://arena.gov.au/assets/2021/03/loganholmewastewater-treatment-plant.pdf (accessed May 9, 2025).

[18] L.J. Winchell, J.J. Ross, M.J. Wells, X. Fonoll, J.W. Norton Jr, K.Y. Bell, Per-and polyfluoroalkyl substances thermal destruction at water resource recovery facilities: a state of the science review, Water Environ. Res., 93 (6) (2021) 826–843, https://doi.org/10.1002/wer.1483.

[19] I.G. Hakeem, P. Halder, S. Patel, E. Selezneva, N. Rathnayake, M.H. Marzbali, G. Veluswamy, A. Sharma, S. Kundu, A. Surapaneni, M. Megharaj, K. Shah, Current understanding on the transformation and fate of per-and polyfluoroalkyl substances before, during, and after thermal treatment of biosolids, Chem. Eng. J. 493 (2024) 152537.

[20] J. Wang, Z. Lin, X. He, M. Song, P. Westerhoff, K. Doudrick, D. Hanigan, Critical review of thermal decomposition of per-and polyfluoroalkyl substances: mechanisms and implications for thermal treatment processes, Environ. Sci. Technol., 56–9 (2022) 5355–5370, https://doi.org/10.1021/acs.est.2c02251.

[21] J. Zhang, L. Gao, D. Bergmann, T. Bulatovic, A. Surapaneni, S. Gray, Review of influence of critical operation conditions on by-product/intermediate formation during thermal destruction of PFAS in solid/biosolids, Sci. Total Environ., 854 (2023) 158796, https://doi.org/10.1016/j.scitotenv.2022.158796.

[22] T. Stoiber, E. Sydney, O.V. Naidenko, Disposal of products and materials containing per-and polyfluoroalkyl substances (PFAS): a cyclical problem, Chemosphere 260 (2020) 127659, https://doi.org/10.1016/j.chemosphere.2020.127659.

[23] B.G. Loganathan, K.S. Sajwan, E. Sinclair, K.S. Kumar, K. Kannan, Perfluoroalkyl sulfonates and perfluorocarboxylates in two wastewater treatment facilities in Kentucky and Georgia, Water Res., 41–20 (2007) 4611–4620, https://doi.org/10.1016/j.watres.2007.06.045.

[24] L.J. Winchell, M.J. Wells, J.J. Ross, F. Kakar, A. Teymouri, D.J. Gonzalez, K. Dangtran, S.M. Bessler, X.F. Almansa, J.W. Norton Jr, K.Y. Bell, Fate of perfluoroalkyl and polyfluoroalkyl substances (PFAS) through two full-scale wastewater sludge incinerators, Water Environ. Res., 96 (3) (2024) e11009, https://doi.org/10.1002/wer.11009.

[25] B.A. Seay, K. Dasu, I. MacGregor, M.P. Austin, R.T. Krile, A.J. Frank, G.A. Fenton, D.R. Heiss, R.J. Williamson, S. Buehler, Per- and polyfluoroalkyl substances fate and transport at a wastewater treatment plant with a collocated sewage sludge incinerator, Sci. Total Environ., 874 (2023) 162357, https://doi.org/10.1016/j.scitotenv.2023.162357.

[26] F. Wang, X. Lu, X.Y. Li, K. Shih, Effectiveness and mechanisms of defluorination of perfluorinated alkyl substances by calcium compounds during waste thermal treatment, Environ. Sci. Technol. 49–9 (2015) 5672–5680, https://doi.org/10.1021/es506234b.

[27] F. Wang, K. Shih, X. Lu, C. Liu, Mineralization behavior of Fuorine in perfuorooctanesulfonate (PFOS) during thermal treatment of lime-conditioned sludge, Environ. Sci. Technol. 47 (2013) 2621–2627, https://doi.org/10.1021/es305352p.

[28] K. Aleksandrov, H.J. Gehrmann, M. Hauser, H. Matzing, D. Pigeon, D. Stapf, M. Wexler, Waste incineration of Polytetrafluoroethylene (PTFE) to evaluate potential formation of per- and Poly-Fluorinated Alkyl Substances (PFAS) in flue gas, Chemosphere 226 (2019) 898e906, https://doi.org/10.1016/j.chemosphere.2019.03.191.

[29] P.H. Taylor, T. Yamada, R.C. Striebich, J.L. Graham, R.J. Giraud, Investigation of waste incineration of fluorotelomer-based polymers as a potential source of PFOA in the environment, Chemosphere 110 (2014) 17e22, https://doi.org/10.1016/j.chemosphere.2014.02.037.

[30] T. Yamada, P.H. Taylor, R.C. Buck, M.A. Kaiser, R.J. Giraud, Thermal degradation of fluorotelomer treated articles and related materials, Chemosphere 61–7 (2005) 974e984, https://doi.org/10.1016/j.chemosphere.2005.03.025.

[31] M.Y. Khan, S. So, G. da Silva, Decomposition kinetics of perfluorinated sulfonic acids, Chemosphere 238 (2020) 124615, https://doi.org/10.1016/j.chemosphere.2019.124615.

[32] P.J. Krusic, D.C. Roe, Gas-phase NMR technique for studying the thermolysis of Materials: thermal decomposition of ammonium perfluorooctanoate, Anal. Chem. 76–13 (2004) 3800e3803, https://doi.org/10.1021/ac049667k.

[33] United States Environmental Protection Agency, 2020b. Per- and Polyfluoroalkyl Substances (PFAS): Incineration To Manage PFAS Waste Streams Technical BRIEF: Innovative Research for a Sustainable Future. https://www.epa.gov/sites/production/files/2019-09/documents/technical_brief_pfas_incineration_ioaa_approved_final_july_2019.pdf.

[34] M. Urciuolo, R. Solimene, P. Ammendola, S. Krusch, V. Scherer, P. Salatino, R. Chirone, O. Senneca, On the agglomeration tendency of carbonaceous fuels in fluidized beds, Fuel 277 (2020) 118187, https://doi.org/10.1016/j.fuel.2020.118187.

[35] A. Cammarota, F. Cammarota, R. Chirone, G. Ruoppolo, R. Solimene, M. Urciuolo, Fluidized bed combustion of pelletized sewage sludge in a pilot scale reactor, Combust. Sci. Technol., 191 (9) (2019) 1661–1676, https://doi.org/10.1080/00102202.2019.1605363.
[36] A. Cammarota, R. Chirone, P. Salatino, R. Solimene, M. Urciuolo, Particulate and gaseous emissions during fluidized bed combustion of semi-dried sewage sludge: effect of bed ash accumulation on NOx formation, Waste Manage., 33–6 (2013) 1397–1402, https://doi.org/10.1016/j.wasman.2013.02.016.
[37] R. Solimene, M. Urciuolo, A. Cammarota, R. Chirone, P. Salatino, G. Damonte, C. Donati, G. Puglisi, Devolatilization and ash comminution of two different sewage sludges under fluidized bed combustion conditions, Exp. Therm. Fluid Sci., 34–3 (2010) 387–395, https://doi.org/10.1016/j.expthermflusci.2009.10.033.
[38] M. Hartman, K. Svoboda, M. Pohořelý, O. Trnka, Combustion of dried sewage sludge in a fluidized-bed reactor, Ind. Eng. Chem. Res. 44 (10) (2005) 3432–3441, https://doi.org/10.1021/ie040248n.
[39] X. Han, M. Niu, X. Jiang, J. Liu, Combustion characteristics of sewage sludge in a fluidized bed, Ind. Eng. Chem. Res. 51 (32) (2012) 10565–10570, https://doi.org/10.1021/ie3014988.
[40] D.H. Lee, R. Yan, J. Shao, D.T. Liang, Combustion characteristics of sewage sludge in a bench-scale fluidized bed reactor, Energ. Fuel. 22 (1) (2008) 2–8, https://doi.org/10.1021/ef700266q.
[41] M. Urciuolo, R. Solimene, R. Chirone, P. Salatino, Fluidized bed combustion and fragmentation of wet sewage sludge, Exp. Therm. Fluid Sci. 43 (2012) 97–104, https://doi.org/10.1016/j.expthermflusci.2012.03.019.
[42] J. Werther, T. Ogada, Sewage sludge combustion, Prog. Energ. Combust., 25 (1) (1999) 55–116, https://doi.org/10.1016/S0360-1285(98)00020-3.
[43] G.R. Jenness, M.K. Shukla, What can Blyholder teach us about PFAS degradation on metal surfaces? Environ. Sci: Adv. 3 (3) (2024) 383–401, https://doi.org/10.1039/D3VA00281K.
[44] I. Glassman, R.A. Yetter, N.G. Glumac, Combustion, Academic press, 2014.